Ecological Indicators 103 (2019) 331–345

Contents lists available at ScienceDirect

Ecological Indicators

journal homepage: www.elsevier.com/locate/ecolind

Original Articles

Effect of natural conditions and mining activities on vegetation variations in arid and semiarid mining regions

Shiliang Liu, Wenping Li*, Wei Qiao, Qiqing Wang, Yanbo Hu, Zhenkang Wang

School of Resources and Geosciences, China University of Mining and Technology, Xuzhou 221116, Jiangsu, China

ARTICLE INFO

Keywords:
Variation in vegetation
NDVI
Mining activities
Sen + Manna–Kendall method
Ecological sensitivity division

ABSTRACT

Variation in vegetation can provide fundamental information about environment and resources management, especially in mining areas with vulnerable ecosystems. Research has demonstrated that vegetation patterns across river basins, plateaus, and mountains have been affected by climate change. However, variation in vegetation caused by natural conditions and mining activities in arid and semiarid mining areas is rarely examined. Using the Yushenfu mining area as a case study, based on the Sen + Mann–Kendall method, spatiotemporal characteristics of variation in vegetation were first analyzed using normal difference vegetation index (NDVI) time series data from 2006 to 2015. For comparison, a traditional linear regression method was applied to characterize NDVI trends, indicating the feasibility of the Sen + Mann–Kendall method. Subsequently, the effect of geomorphology, groundwater depth, and drought index on NDVI was assessed. The same geomorphology or groundwater depth did not correspond to a specific NDVI value, and a relationship between the drought index and NDVI was obtained. Then, unexploited areas and mined areas were compared, revealing that mining activities have a very obvious negative impact on vegetation ecology. Furthermore, the buried depth of the ecosafety groundwater table was determined to be 1.5–5.0 m based on the curve describing the relationship between groundwater depth and NDVI. This analysis produced an ecological sensitivity map with four key zones: primary, secondary, and tertiary sensitive areas and non-sensitive areas. These results provide a theoretical basis for developing fair and equitable outcomes for mineral resource development and environmental protection.

1. Introduction

As the major organisms dominating terrestrial ecosystems, plants connect nutrient cycling and energy flow among the pedosphere, hydrosphere, and atmosphere (Vereecken et al., 2010). Accordingly, vegetation plays an important role in global change research and the assessment of ecological environments. Natural conditions and strong human activities are changing vegetation conditions, which can lead to vegetation degradation and thus cause soil deterioration (Marques et al., 2008), desertification (Symeonakis and Drake, 2004), and declines in land productivity (Lantican et al., 2003; Pimentel and Kounang, 1998; Xu et al., 2017) and ecological function (Demir et. al., 2017; Liu and Meng, 2018; Rusanov, 2014; Wang et al., 2018a,b; Xie and Zhang, 2018), especially in arid and semiarid zones, where landscape ecologies are very fragile owing to limited water resources. Therefore, it is important to study the effects of natural conditions and human activities on vegetation ecology in order to better regulate human activities and guide the development of ecological environments.

Numerous studies focusing on variation in vegetation have achieved fruitful results (Chen and Wang, 2009; Jiang et al., 2015; Jin et al., 2014; Liu et al., 2018e,f; Tong et al., 2016; Turner, 1990; Yang et al., 2005; Zhang et al., 2011; Zhao et al., 2018). For example, the regional normal difference vegetation index (NDVI) in the northern hemisphere between 40° and 70° N shows a significant upward trend (Ringrose et al., 2002), and the response of vegetation to climate change often lags (Zhou et al., 2002). In addition, variation in vegetation is impacted by annual rainfall (Areola and Fasona, 2018), soil moisture content (Wang et al., 2018a,b), hydrological parameters (Xu et al., 2018), grazing (Chi et al., 2018), and China's ambitious Grain for Green Program (Zhao et al., 2017), each of which has been examined using NDVI. A multi vegetation index-based mixture model was developed to estimate fully covered vegetation and bare soil vegetation indexes (Mu et al., 2018); this model was subsequently used to estimate fractional vegetation cover and compared with the NDVI method for detecting vegetation growth status. Global trend analyses of the main vegetation

* Corresponding author at: School of Resources and Geosciences, China University of Mining and Technology, 1 #University Road, Quanshan District, Xuzhou City, Jiangsu Province, China.
E-mail address: skd571721@126.com (W. Li).

https://doi.org/10.1016/j.ecolind.2019.04.034
Received 18 July 2018; Received in revised form 30 March 2019; Accepted 11 April 2019
Available online 16 April 2019
1470-160X/ © 2019 Elsevier Ltd. All rights reserved.

types were conducted using the latest version of the GIMMS NDVI data set corresponding to the period of January 1982 to December 2015 (Faour et al., 2018). Additionally, a dynamic model was presented to investigate how vegetation patterns are generated and affected by wind in arid and semi-arid areas (Zhang et al., 2017a–c). The aforementioned studied sites were mainly focused on agricultural fields, and variation in vegetation of urban zones was also studied. For example, the spatiotemporal variation in surface temperatures of Ahmedabad, India and its relationship with vegetation and urbanization parameters as indicators of surface temperatures were investigated (Mathew et al., 2018). Variation in the relationship among urban vegetation, surface temperature, and air temperature was examined at micro- and regional-scales (Shiflett et al., 2017).

Moreover, vegetation is an important indicator of ecological environments. Thus, the ecological vulnerability of vegetation can be assessed, and a zoning map of different degrees of impact to the ecological environment can be obtained, which can guide ecological environment protection and management (He et al., 2018; Wan et al., 2018; Zhang et al., 2017a–c). Additionally, most research sites for studies on the effects of climate change and human activities on vegetation ecology are river basins, mountains, or plateaus (Wang et al., 2015; Xin et al., 2008; Zhang et al., 2016a,b). In the upper basin of the Yellow River, a field study showed that hygrophytes were gradually replaced by mesophytes, xerophytes, and some annual psammophilous plants; additionally, cover and herbaceous biomass decreased along with the progressive desertification (Wang et al., 2007). The spatiotemporal variation and sustainability of vegetation coverage and was also recently characterized, as was the relationship between vegetation NDVI and climatic factors in the wet season in the Red River Basin (Gu et al., 2018). Similarly, in the Loess Plateau region of China, climate variability and human activities have both contributed to vegetation changes, among which human activities account for 55% of vegetation changes over 2000–2015 (Li et al., 2017a,b). Additionally, long-term changes over the past 30 years in the areas and vegetation coverage of lakes in the Qinghai-Tibetan Plateau and their relations to the climate change were analyzed (Zhang et al., 2018). In contrast to the effect of climate change on vegetation, human activities have played a major role in vegetation variation law (Liu et al., 2018e,f; Sun et al., 2015). Among studies of the influence of human activities, the effect of groundwater extraction and land use on vegetation changes have been most extensive (Elmore et al., 2006; Jeevarathinam et al., 2013; Sun et al., 2008; Tasser and Tappeiner, 2002). Additionally, the effect of mining activities on vegetation ecology has also been studied (Musa and Jiya, 2011; Tian et al., 2013), but no comparative studies have been conducted in mined areas and un-mined mineral-rich areas.

The aforementioned research results have important guiding significance for the development of ecosystems and sustainable socioeconomic development at regional or global scales. Several great shifts are occurring in coal mining throughout China: from Middle East China to Northwest China, from humid and semi-humid to arid and semiarid mining areas, from deep to shallow mining depth, from low to high intensity mining of coal seams, from geomorphological types such as hills or plains to plateaus or deserts, and from less to more likely to leak phreatic water resources. Overall, these shifts have increased the fragility of the vegetation ecological environment, relative to the previous impacts on the eastern mining areas of China, especially in arid and semiarid mining regions (Lei and Bian, 2014; Wang, 2017). On the basis, geomorphology, groundwater depth, climate conditions, and mining activities are selected as the influence factors on vegetation changes in arid and semiarid mining regions. Furthermore, quantitative relationships between NDVI and geomorphology, climate conditions, or groundwater table were rarer, the quantitative effect of mining activities on vegetation changes and the non-significant trend of NDVI was not identified in previous studies.

Therefore, the main objective of the paper was to study the effect of geomorphology, groundwater depth, climate conditions, and mining activities on variation in vegetation across arid and semiarid mining regions. More specifically, spatiotemporal characteristics of variation in vegetation were first analyzed using NDVI time series data from 2006 to 2015 based on the Sen + Mann–Kendall method. In order to verify the feasibility of the Sen + Mann–Kendall method, a simple linear regression method was applied to describe NDVI trends. Then, the effect of geomorphology, groundwater depth, and drought index on NDVI was assessed. Comparative analyses were conducted on variation in vegetation affected by mining activities between mined areas and unexploited areas with potential for mining. Finally, an ecological sensitivity map was obtained with four zones based on the buried depth of the eco-safety groundwater table. Our results will contribute to establishing mineral resources development and ecological environment protection in order to provide optimal benefits to all parties and the environment.

2. Materials and methods

2.1. Study site

Jurassic Coalfield in Northern Shaanxi, an arid to semi-arid region, is one of the seven largest coalfields in the world, accounting for about 25% of China's proven coal reserves. The Yushenfu mining area, a typical mining area in the North Shaanxi Jurassic Coalfield, which includes the Yushen and Shenfu mining areas, is located in the northern part of Yulin City, Shaanxi Province, China, and its total area is about 6334 km^2, as shown in Fig. 1. Moreover, the Yushenfu mining area, with proven coal reserves of 147 billion tons, is an important energy and heavy chemical industry base in China. In addition, water resources in the region are scarce, natural vegetation is sparse, and the surface vegetation coverage is low. The study area was selected based on these features. The geographic coordinates of the study area are as follows: longitude, 109° 08′ 24″ E–110° 27′ 59″ E; latitude, 38° 19′ 33″ N–39° 11′ 23″ N. The Yushen mining area consists of four planning areas, the # 1, # 2, # 3, and # 4 planning areas. The # 1 and # 2 planning areas and the Shenfu mining area have been exploited on a large scale, while the overall planning of the # 4 planning area is still being developed. Additionally, the study area is located on the border of the Maowusu Desert and the Loess Plateau, which has a continental monsoon climate in its arid and semi-arid regions. The vegetation ecology is the primary protection target for the study area, and the groundwater source that directly affects the vegetation ecology is a phreatic aquifer occurring at a shallow depth. The phreatic aquifer, which has ecological significance and is capable of supplying water to widely distributed localities within the study area, is widely distributed throughout the region. Plants can be divided into aquatic and terrestrial plants according to their dependence on water. Terrestrial plants can then be divided into hygrophytes, mesophytes, and xerophytes (Zhang and Dang, 2014). According to this classification scheme, the vegetation types are mainly xerophytes in the study area, such as *Achnatherum splendens*, sand sagebrush, and *Salix mongolica*. The hygrophytes and mesophytes exist only in local areas with shallower buried depths of the phreatic water table, including white thorn, reeds, and licorice as well as halophytic meadow, swampy meadow, and swampy shrub vegetation.

2.2. Data sources

The datasets used in the paper comprise NDVI data, precipitation data, evaporation data, drought index data, phreatic water table depth, and geomorphology types.

NDVI data are comprised of ratios of the difference between near infrared and red reflectance to the sum of near-infrared and red reflectance, which is recognized as the most commonly used remote sensing data for the characterization of vegetation change. NDVI datasets have been widely used to describe vegetation dynamics because of their close correlation with biophysical and biochemical variables

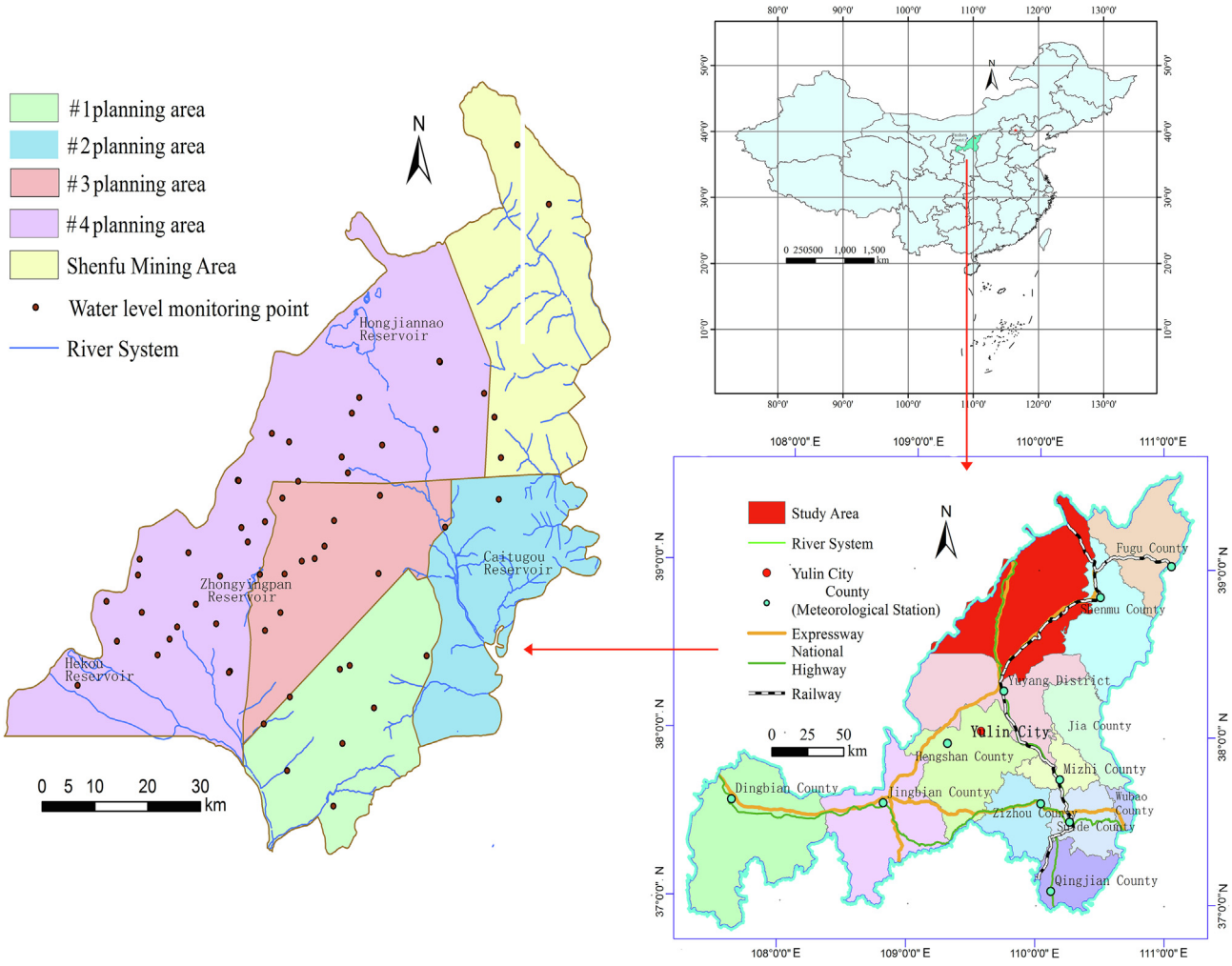

Fig. 1. Location of the study site.

(Zhang et al., 2016a,b). The NDVI datasets used in this study are comprised of MODIS (MOD 13) NDVI data, which were downloaded from NASA's Earth Observing System. The dataset is provided by the National Earth System Science Data Sharing Infrastructure (http://www.geodata.cn/). The spatial resolution of MODIS NDVI data is 250 m, and the time series spans 10 years, from 2006 to 2015. According to field investigations, the most vigorous vegetation growth occurs from July to October. Hence, the annual maximum NDVI data are used to represent vegetation coverage conditions for each year. There are seven images each year, with a total of seventy images during the 2006–2015 period.

The observed monthly precipitation and evaporation datasets used in this study were provided by the National Meteorological Information Center of the China Meteorological Administration (http://data.cma.cn). The site-based datasets for precipitation and evaporation were obtained from 18 meteorological station observations from 2006 to 2015 in Yulin City (Fig. 1). Furthermore, the drought index, an indicator of drought, is defined as the ratio of annual evaporation to annual precipitation. In order to reflect the impact of rainfall and evaporation on vegetation comprehensively, the drought index r is used as a climate indicator. The formula used to calculate the drought index is (Liu, 1999)

$$r = E_O/P = kE_p/P \quad (1)$$

where E_o is the multi-year mean value of the actual water surface evaporation, in mm; E_p is the multi-year mean value of evaporation observed in an evaporating dish, in mm; P is the average annual rainfall, in mm; and k is the correction coefficient of the evaporating dish. In this paper, $k = 0.55$ (Shi et al., 1986).

The depth of groundwater, the distance between the surface and ground water table, is not only the key index for diagnosing the health of the ecosystem in arid areas (Kopeć et al., 2013; Li et al., 2016, 2017a,b) but is also an important method for revealing the water requirements of vegetation (Christoffersen et al., 2014). The phreatic water table depth data were obtained from 59 water-level observation stations (Fig. 1), and the monitoring method has been previously described (Fan et al., 2016). The overall terrain of the study area is high in the northwest and low in the southeast (Pei, 2017). Topography data, originating from digital elevation model (DEM) data, which are three-dimensional computer graphic representations of terrain surfaces, were classified in ArcMap version 10.1 software (Minami et al., 2000; Mou, 2012).

2.3. Methods

2.3.1. Trend analysis

2.3.1.1. Simple linear regression method. Simple linear regression is an important method for studying temporal variation of vegetation, in which time series data conform to a normal distribution and are vulnerable to noise. For NDVI time series data, the simple linear regression equation for time − independent variable x and NDVI − dependent variable y is obtained using the least squares method (Lu, 2007), where slope k represents the change in vegetation. Generally, $k > 0$ indicates vegetation was improved,

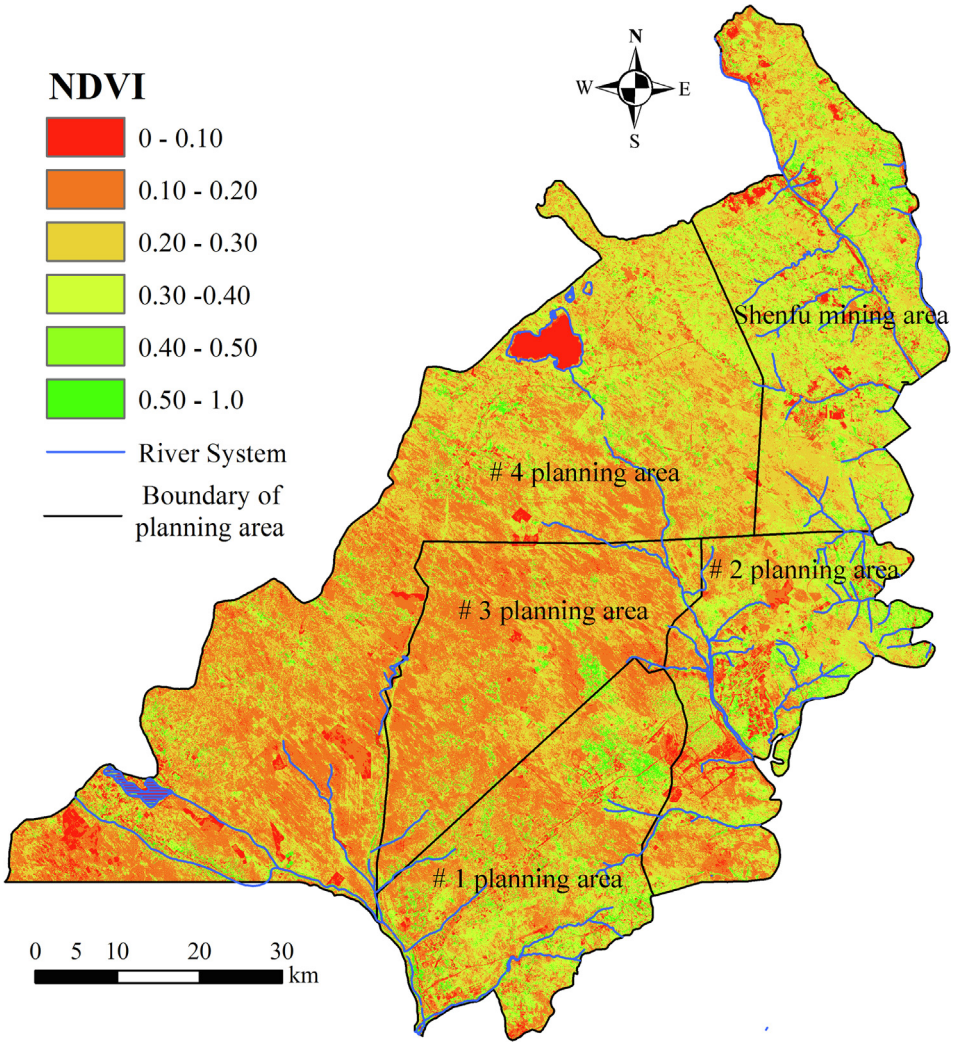

Fig. 2. The distribution of 2014 normal difference vegetation index (NDVI) average values in the Yushenfu mining area.

while $k < 0$ indicates vegetation was degraded. The calculation method for slope k is shown in Eq. (2).

$$k = \frac{\sum_{i=1}^{n}(x_i - \bar{x})(y_i - \bar{y})}{\sum_{i=1}^{n}(x_i - \bar{x})^2} \tag{2}$$

where k is the slope of the single linear regression equation; $\bar{x} = \frac{1}{n}\sum_{i=1}^{n} x_i$; $\bar{y} = \frac{1}{n}\sum_{i=1}^{n} y_i$; $n = 10$; x_i is a time series data point at time i; y_i is a NDVI series data point for time i.

In the study, 10 data sets (x_i, y_i values) were first extracted and computed separately to obtain the k values in each grid cell. Subsequently, $\bar{x}$ and $\bar{y}$ were calculated. Finally, NDVI trends were divided into three categories in ArcGIS, i.e., decreases, gentle fluctuations, and increases, and the corresponding k values were < -0.005, -0.005–0.005, and > 0.005, respectively.

2.3.1.2. Sen + Mann–Kendall method. Sen trend degree and Mann − Kendall trend tests have become an important method for judging trends in time series data. Sen's slope was calculated from median time series data, which can reduce noise interference very well, but it cannot be used to determine the significance of a temporal trend. In addition, the Mann–Kendall method has no requirements for temporal distributions and is insensitive to outliers (Stow et al., 2003; Song et al., 2011; Kong et al., 2018). Therefore, the combination of Sen trend analysis and a Mann–Kendall test can effectively predict trends in long time series datasets and, to a certain extent, improve the accuracy of analysis results.

In this study, Sen trend analysis was used to analyze the spatial distribution characteristics of long NDVI time series. The formula for Sen trend analysis is (Sen, 1968)

$$Slope = Median\,[(NDVI_j - NDVI_i)/(j - i)], \qquad \forall\, j > i \tag{3}$$

where i and j represent time series indexes, $NDVI_j$ and $NDVI_i$ are the NDVI values of time series in pixels j and i, respectively. When Slope > 0, NDVI exhibits an upward trend; when Slope < 0, NDVI exhibits a downward trend.

The Mann–Kendall test is a nonparametric statistical test that is used to detect the significance of trend changes. This method is widely used in the analysis of long time series. The formulas for this method are (Kendall, 1970; Tosic, 2004)

$$S = \sum_{i=1}^{n=1}\sum_{j=i+1}^{n} \mathrm{sgn}(NDVI_j - NDVI_i) \tag{4}$$

$$\mathrm{sgn}(NDVI_j - NDVI_i) = \begin{cases} 1 & (NDVI_j - NDVI_i > 0) \\ 0 & (NDVI_j - NDVI_i = 0) \\ -1 & (NDVI_j - NDVI_i < 0) \end{cases} \tag{5}$$

where $NDVI_j$ and $NDVI_i$ are the NDVI values of the time series for pixels j and i, respectively, n is the length of the time series, sgn() is a sign function, and S is the test statistic.

Because of the difference in the n values of the time series lengths,

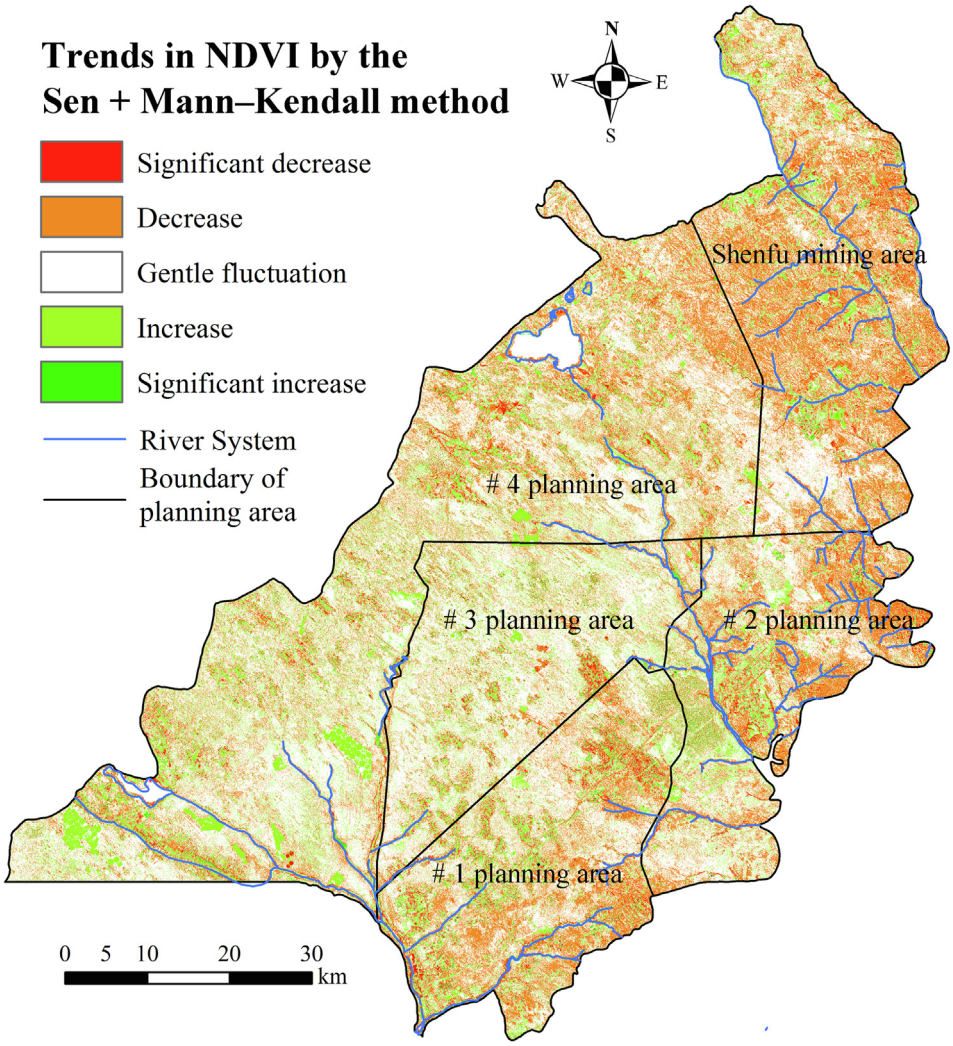

Fig. 3. Trends in normal difference vegetation index (NDVI) by the Sen + Mann–Kendall method from 2006 to 2015 in the Yushenfu mining area.

Table 1
Statistical results of normal difference vegetation index (NDVI) trends using the Sen + Mann–Kendall method.

Variation trend	Area/km^2	Percentage of area/%
Significant decrease	323	5.10
Decrease	519	8.19
Gentle fluctuation	3510	55.41
Increase	1380	21.78
Significant increase	603	9.52

the appropriate statistical test for inferring significance differs. When $n < 10$, the test statistic S is used directly for a bilateral trend test. If $S > 0, S = 0$, or $S < 0$, an upward trend, lack of trend, or a downward trend, respectively, are supported. When n ≥ 10, the statistic S obeys the standardized normal distribution, and the test statistic Z is used as the test of trend significance. The Z value is calculated according to Eqs. (6) and (7),

$$Z = \begin{cases} (S-1)/\sqrt{s(S)}, & S > 0 \\ 0, & S = 0 \\ (S+1)/\sqrt{s(S)}, & S < 0 \end{cases} \quad (6)$$

$$s(S) = n(n-1)(2n+5)/18 \quad (7)$$

where Z is a test statistic, s is the variance, and n is the length of the time series. Given confidence level α, $|Z| > Z_{1-\alpha/2}$ indicates that there are significant changes in the sequence.

In this study, the time series was of length $n = 10$, so the test statistic Z was used to examine the trend. The confidence level was $\alpha = 0.05$, that is, $Z_{1-\alpha/2} = Z_{0.975} = 1.96$. For non-significant changes, some of the trends nearly exhibited no change. At this time, if the NDVI of nearly no change in grid cells are also added to the corresponding increasing or decreasing trend, it will cover the smoothness of this kind of pixel change. Additionally, the annual variability of NDVI changed between −0.005 and 0.008, which is regarded as essentially unchanged vegetation growth (Mao et al., 2007). Hence, for the convenience of calculation, ± 0.005 was chosen as the threshold, and slope values between −0.005 and 0.005 are henceforth described as a gentle fluctuation.

Accordingly, five kinds of classification results were obtained through trend and significance analyses: (1) Slope < -0.005 & $|Z| > 1.96$ indicates a “significant decrease” trend; (2) Slope < −0.005 & $|Z| \leqslant 1.96$ indicates a “decrease” trend; (3) −0.005 ≤ Slope ≤ 0.005 indicates a “gentle fluctuation” trend; (4) Slope > 0.005 & $|Z| \leqslant 1.96$ indicates an “increase” trend; (5) Slope > 0.005 & $|Z| > 1.96$ indicates a “significant increase” trend.

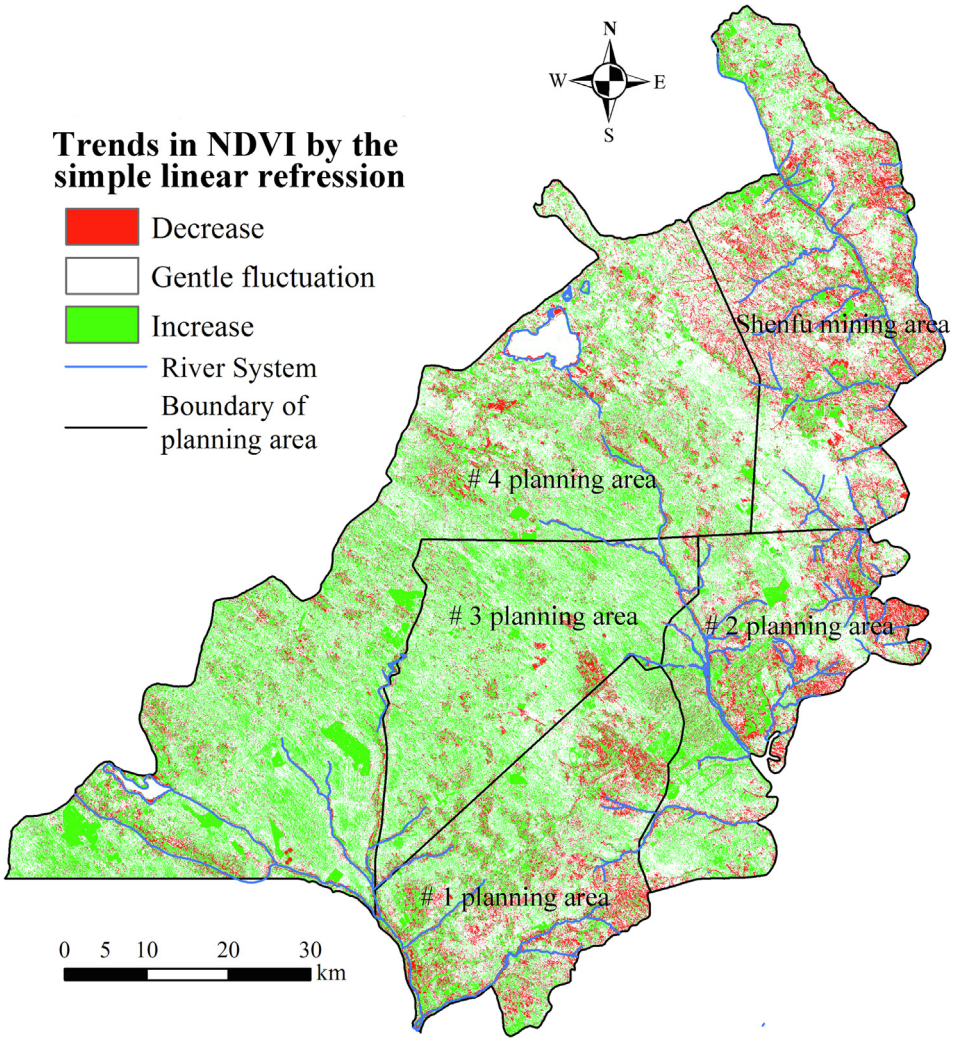

Fig. 4. Trends in 2006–2015 normal difference vegetation index (NDVI) assessed by linear regression in the Yushenfu mining area.

Table 2
Statistical summary of normal difference vegetation index (NDVI) trends based on simple linear regression.

Trend	Area (km^2)	Percentage of area (%)
Decrease	647	10.21
Gentle fluctuation	3447	54.41
Increase	2241	35.38

2.3.2. Data processing method

To further eliminate the influence of cloud cover, atmospheric conditions, and solar altitude angle, the NDVI datasets were pre-processed to provide atmospheric, radiometric, and geometric corrections using ENVI software (Deng, 2014; Chen et al., 2017a, b). Subsequently, the Maximum Value Composite method was used to obtain the annual maximum NDVI among the seven images corresponding to each year in ArcMap version 10.1 (Minami et al., 2000; Mou, 2012), which was used to represent vegetation changes over each year. Then, the boundary of the study area was used to remove the Yushenfu Mining Area NDVI data. Finally, the spatiotemporal characteristics of NDVI, the relationships among geomorphology, groundwater depth, drought index, and NDVI were obtained, and the effect of mining activities on NDVI as well as the buried depth of the eco-safety groundwater table was explored according to the following steps.

(1) In view of the limited space and the large number of pictures in the study, the 2014 NDVI average values were used to characterize the spatial distribution characteristics of vegetation. Subsequently, based on the Mann–Kendall and Sen's slope method, the vegetation trend analysis was conducted on the MATLAB platform. Combined with the ArcMap spatial analysis function, the trend in average NDVI values in the Yushenfu mining area during the period of 2006 to 2015 was obtained. Additionally, in order to verify the feasibility of the Sen + Mann–Kendall method, a simple linear regression method was applied to describe NDVI trends.
(2) The study area was divided into a grid of 250 × 250 m cells using the square regular mesh generation method in ArcGIS (Mou, 2012; Liu et al., 2018b).
(3) On the basis of geomorphology types and the distribution characteristics of the study area, NDVI mean values of grid cells under different geomorphic types were computed and the relationship between NDVI values and geomorphic types were obtained.
(4) According to the water level monitoring data, the mean NDVI values of different depths of phreatic water were computed for each grid cell. Furthermore, the relationship between the depth of phreatic water and mean NDVI values was investigated.
(5) According to the monthly precipitation and evaporation data during the period of 2006 to 2015, the average annual rainfall was calculated (for data, see Supplementary file). The ordinary Kriging method implemented in ArcMap version 10.1 (Minami et al., 2000;

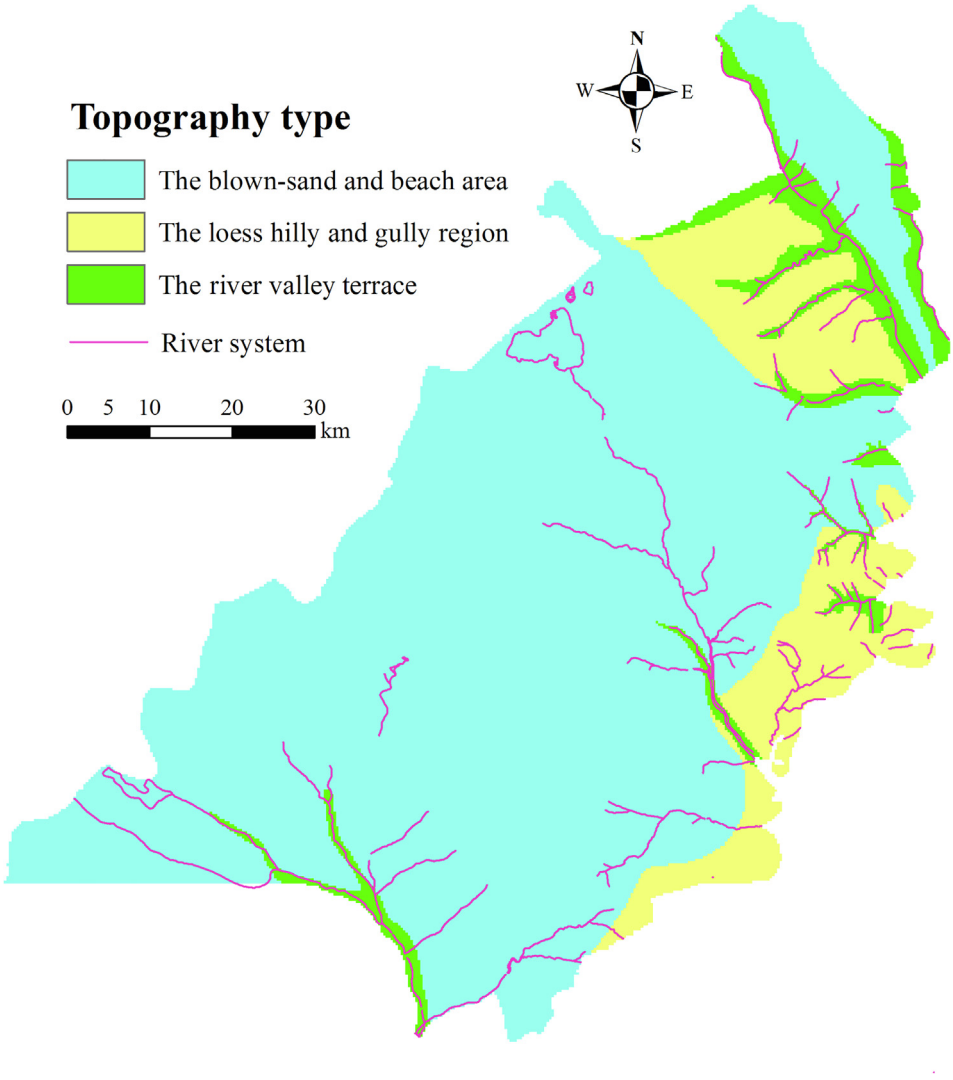

Fig. 5. Topography types.

Table 3
Relationships among geomorphic types, areas and location.

Geomorphic types	Area /km^2	Percentage of area/%	Location
Blown-sand and beach area	5073	80	the northwest area of the study area
Loess hilly and gully region	857	14	the eastern region of the study area
River valley terrace	381	6	near the surface water system of the study area

Mou, 2012; Gruijter et al., 2006; Webster and Oliver, 2008) was used to interpolate a thematic map of meteorological datasets. For consistency with the NDVI data, the meteorological thematic map was resampled to a spatial resolution of 250 m and transformed to the same coordinate system (Projected coordinate system: Beijing_1954_GK_Zone_19). Subsequently, the contour of the drought index was also obtained based on Eq. (1). Then, the drought index value in each grid cell was extracted. The drought index had 0.1 m increments, and the mean NDVI values within each grid cell were geometrically averaged. Finally, the quantitative relationship between drought index and mean NDVI values was analyzed using the least squares method (Lu, 2007).

(6) In order to study the influence of coal mining on vegetation ecology, the NDVI trends in the # 4 planning area of the Yushen mining area (an un-mined area) and Shenfu mining area (a currently mined area) were selected for comparison. Furthermore, the different NDVI disturbance levels in the # 4 planning area of the Yushen mining area and the Shenfu mining area were compared, and the percentages of area demonstrating decreases, no change, and increases were separately calculated in the mined and un-mined areas.

(7) From the perspective of sustainable development, the buried depth of eco-safety on groundwater table refers to the depth of the groundwater table that maintains the normal growth of vegetation and the normal ecological functions of rivers, lakes, and marshes without causing desertification and deterioration of water quality in arid and semi-arid areas (Yang et al., 2006). In order to determine the buried depth of the eco-safety groundwater table, first, a scatter plot of the depth of the groundwater table and mean NDVI values was drawn. Subsequently, in order to obtain the quantitative relationship between the buried depth of the groundwater table and mean NDVI values, the buried depth of the groundwater table was

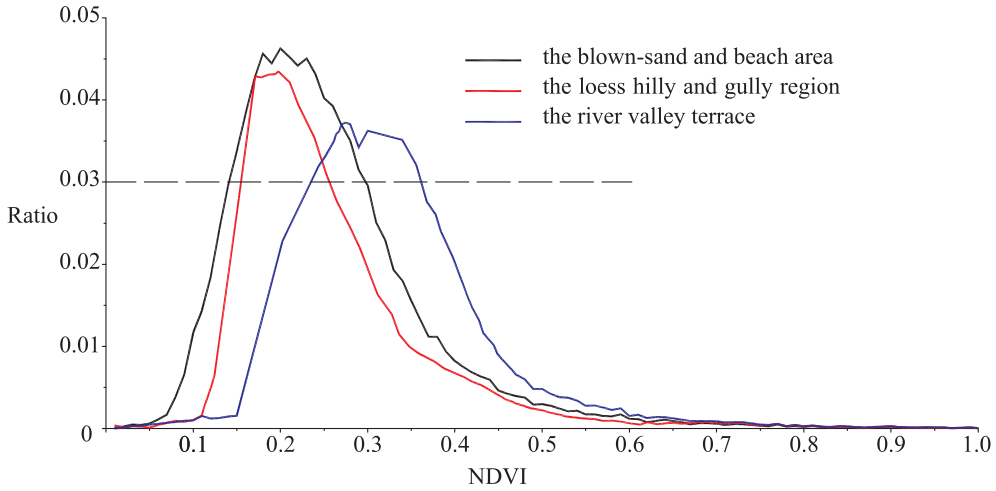

Fig. 6. Relationship between geomorphic types and normal difference vegetation index (NDVI) values.

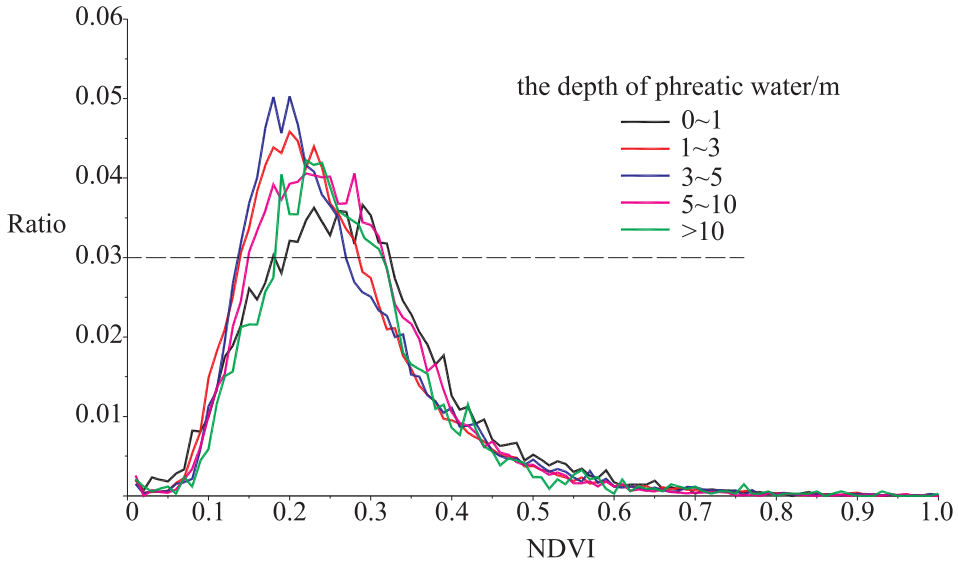

Fig. 7. Relationship between the depth of phreatic water and normal difference vegetation index (NDVI) values.

Table 4
Relationships between depth of phreatic water and mean normal difference vegetation index (NDVI) values.

Buried depth of phreatic water/m	NDVI	Buried depth of phreatic water/m	NDVI	Buried depth of phreatic water/m	NDVI
0–1	0.18–0.33	1–3	0.14–0.28	3–5	0.14–0.26
5–10	0.15–0.32	greater than10	0.18–0.32		

determined at 0.1-m intervals, and then mean NDVI values within each range of groundwater table depths were geometrically averaged. Finally, the quantitative relationship between drought index and NDVI was obtained using the least squares method (Lu, 2007).

3. Results

3.1. Spatiotemporal characteristics of NDVI

3.1.1. Spatial characteristics of NDVI

Fig. 2 shows the spatial distribution of 2014 NDVI average values in the Yushenfu mining area. The areas with NDVI average values greater than 0.3 were mainly concentrated in river basins, the Yushen mining area, the southeastern part of the # 1 planning area, the northeastern part of the # 2 planning area, and the 4# planning area. The areas with NDVI average values less than 0.3 were mainly concentrated in the northwest part of the # 1 planning area, the southeastern part of the # 2 planning area, the # 3 planning area, and the southwestern part of the # 4 planning area. Among them, the NDVI average values of the # 3 planning area were mainly between 0.1 and 0.2. In general, the NDVI value is small and the vegetation coverage is low in the Yushenfu mining area, which is affected by natural conditions and mining activities.

3.1.2. Temporal trends in NDVI

Fig. 3 shows trends in NDVI by the Sen + Mann–Kendall method from 2006 to 2015 in the Yushenfu mining area. The areas exhibiting “gentle fluctuations” account for the majority of areas, which are mainly distributed in the # 3 and # 4 planning areas of the Yushen mining area. The areas of vegetation degradation were mainly

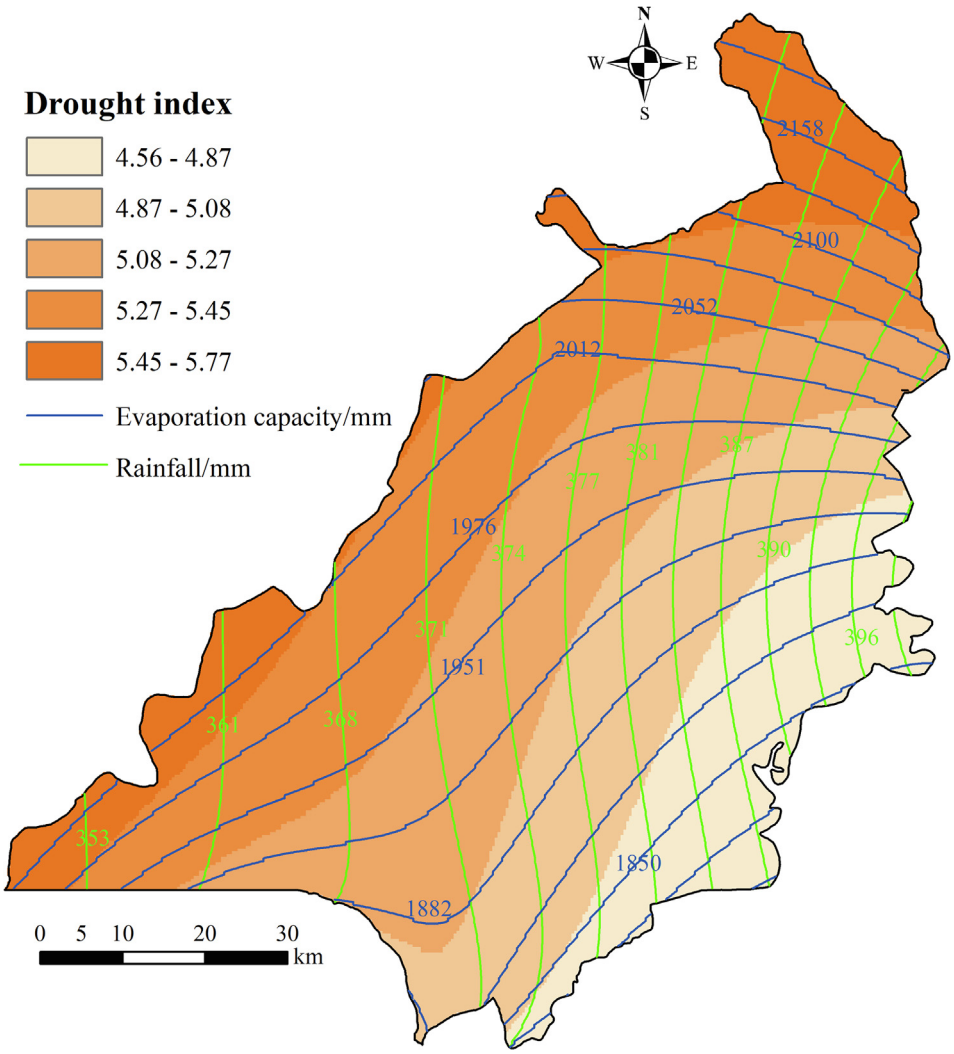

Fig. 8. Contours of rainfall, evaporation, and the drought index.

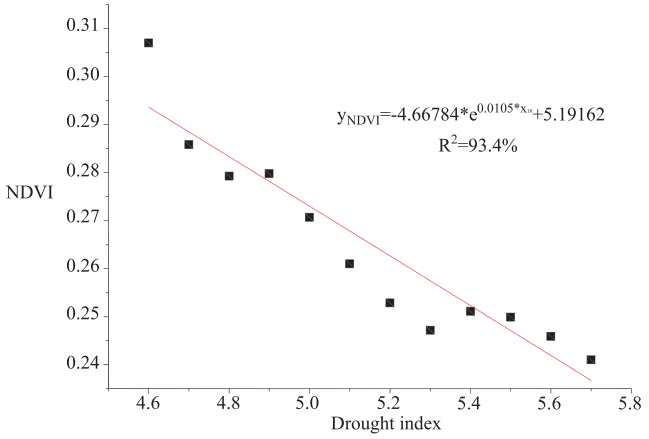

Fig. 9. The relationship between drought index and normal difference vegetation index (NDVI) values.

distributed in the # 1 and # 2 planning areas of the Yushen mining area and the Shenfu mining area, where considerable mineral resources have been exploited on a large scale. The statistical results of the NDVI trends during the 2006–2015 period in the study area are listed in Table 1, showing an upward NDVI trend from 2006 to 2015 in the study area.

For comparison, Fig. 4 shows the 2006–2015 NDVI trend using simple linear regression for the Yushenfu mining area. Furthermore, a statistical summary of NDVI trends is shown in Table 2. Comparison of the NDVI trends using the Sen + Mann–Kendall and simple linear regression reveals that the overall trends in NDVI are consistent, but there are slight differences in NDVI increases, decreases, and fluctuations in area percentages. Specifically, the differences in area percentages of NDVI decreases, fluctuations, and increases are 3.08%, 1%, and 4.08%, respectively. Through comparative analysis, NDVI trends captured by the Sen + Mann–Kendall method are reasonable.

3.2. Effect of natural conditions on NDVI

3.2.1. Geomorphology

Fig. 5 shows the three major geomorphic types in the study area, namely, the blown-sand and beach area, the loess hilly and gully region, and the river valley terrace. Furthermore, Table 3 exhibits relationship among geomorphic types, areas and location.

Fig. 6 shows the relationship between NDVI values and geomorphic types. The longitudinal axis in Fig. 6 presents a percentage of NDVI values across different geomorphic types. In Fig. 6, different geomorphic types correspond to different NDVI value distributions, and the same geomorphology does not correspond to a determined mean NDVI value but is almost always distributed from 0 to 1. The mean NDVI value of different geomorphic types shows obvious patterns. Taking NDVI ratios greater than 0.03 as an example, the mean NDVI values in

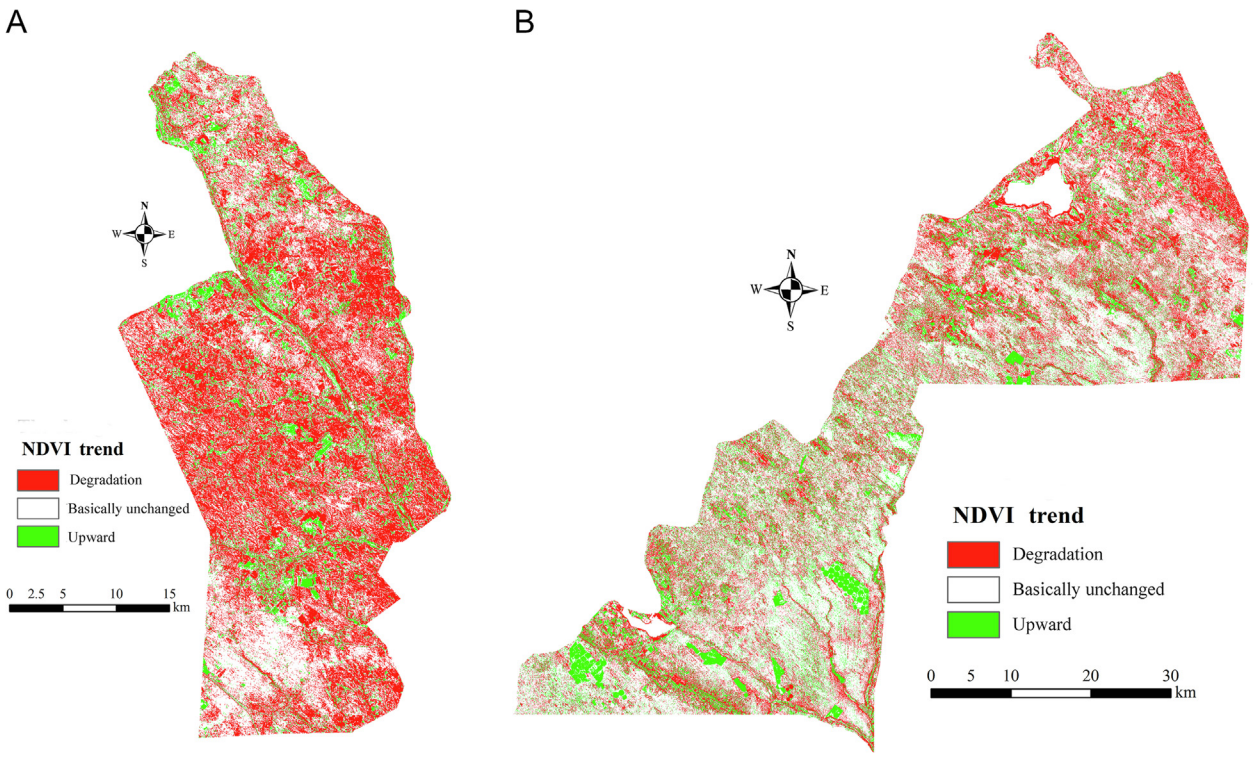

Fig. 10. Normal difference vegetation index (NDVI) trend in the Shenfu mining area and the # 4 planning area of the Yushen mining area: (a) the Shenfu mining area (b) the # 4 planning area of the Yushen mining area.

Table 5
Statistical summary of the influence of coal mining on vegetation ecology.

Variation trend	Shenfu mining area (mined mining area)		the # 4 planning area of Yushen mining area (unexploited area)		Percentage difference (%)
	Area (10^8 m^2)	Percentage (%)	Area (10^8 m^2)	Percentage (%)	
Degradation	5.296833	46.0158	6.386697	25.0889	20.9269
Basically unchanged	5.031531	43.7110	15.352749	60.3104	−16.5990
Upward	1.182537	10.2732	3.716793	14.6007	−4.3275

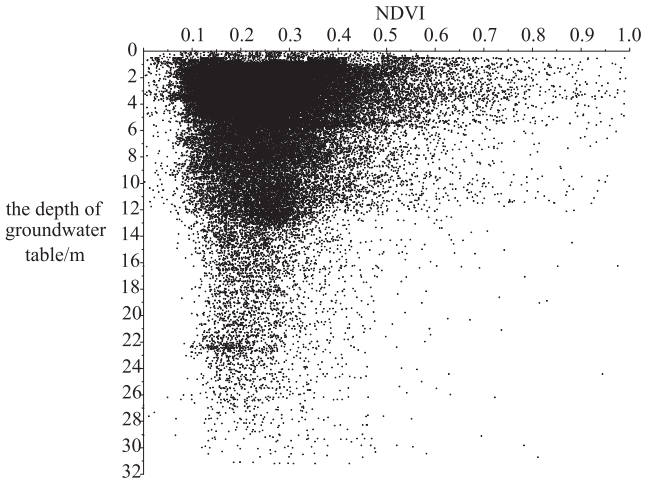

Fig. 11. Scatterplot of the depth of groundwater table and normal difference vegetation index (NDVI) values.

the blown-sand and beach area, loess hilly and gully region, and river valley terrace were 0.14–0.29, 0.16–0.26, and 0.24–0.36, respectively, showing that the overall NDVI values also increases gradually, as shown in Fig. 6. In general, geomorphological types play an important role in controlling the spatial distribution and growth of vegetation.

3.2.2. Groundwater depth

Fig. 7 shows the relationship between the depth of phreatic water and mean NDVI values based on 2014 water level data. The longitudinal axis in Fig. 7 presents the percentage of mean NDVI values for different depths of phreatic water. It is concluded that different depths of phreatic water correspond to different mean NDVI value distributions, and the same depth of phreatic water does not correspond to a determined mean NDVI value, but is almost always distributed from 0 to 1.

The mean NDVI values of different depths of phreatic water show obvious patterns. Taking the NDVI ratio greater than 0.03 as an example, Table 4 shows relationships between depth of phreatic water and mean NDVI values. The overall mean NDVI values gradually decreased in the areas with groundwater depths of 0–5 m, which reflects the deterioration of the vegetation ecology. Compared with the NDVI values of groundwater depths of 3–5 m, the mean NDVI values showed an upward trend in areas with groundwater depths of 5–10 m. When the groundwater depth is greater than 10 m, compared with the NDVI values of groundwater at depths of 5–10 m, the mean NDVI value is basically unchanged. Thus, vegetation growth is independent of groundwater when the groundwater level is greater than a certain depth, which supports previous results (Zhang and Dang, 2014).

3.2.3. Drought index

Fig. 8 shows the contours of rainfall, evaporation, and the drought

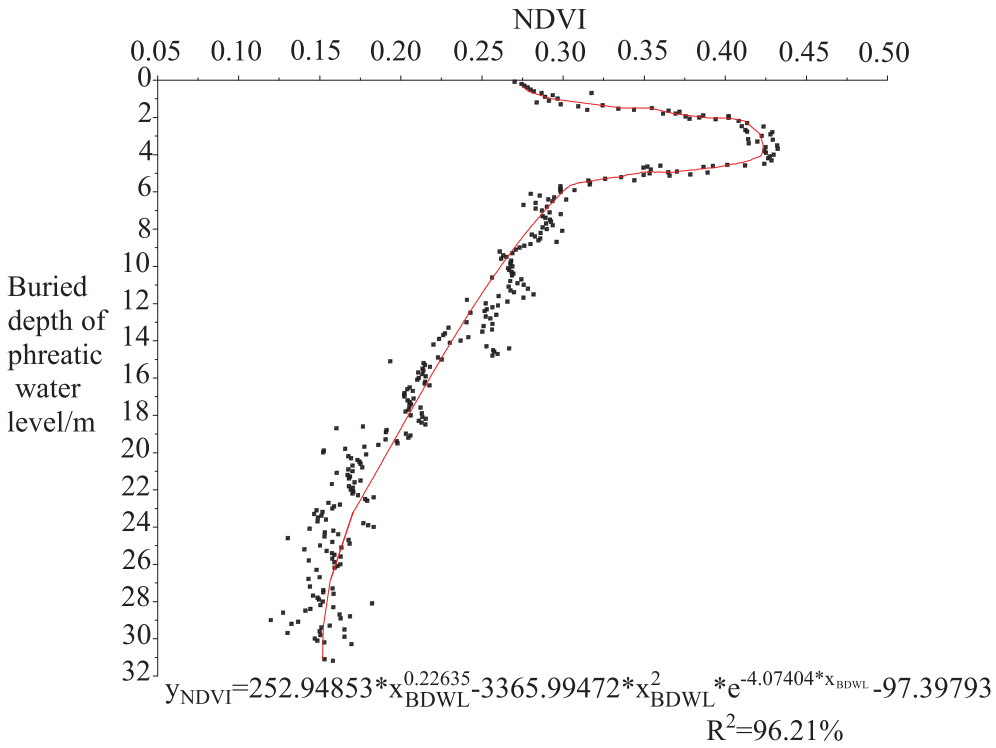

Fig. 12. Curve describing the relationship between groundwater depth and normal difference vegetation index (NDVI) values.

index. The drought index was 4.56–5.77 in the Yushenfu mining area. According to the climate classification criteria (United Nations Educational Scientific and Culture Organization, 1979; United Nations Environment Programme, 1992), a drought index of 2–5 corresponds to a semi-arid climate. A drought index more than 5 corresponds to an arid climate. Accordingly, the study area has an arid to semiarid climate. Furthermore, the quantitative relationship between drought index and mean NDVI values is shown in Eq. (8) and Fig. 9.

$$y_{NDVI} = -4.66784 \cdot e^{0.0105 x_{DI}} + 5.19162 \quad (8)$$

The correlation coefficient $R^2 = 0.934$, where y_{NDVI} is NDVI and x_{DI} is the drought index.

In summary, the temporal variation of vegetation is the manifestation of the comprehensive effects of climate conditions, while the spatial heterogeneity is mainly affected by geomorphology. Moreover, geomorphology can influence climate types by affecting atmospheric circulation, evaporation and heat dissipation in a region; meanwhile, geomorphology also influences the depth and flow field of groundwater. Therefore, natural conditions play an important role in controlling the ecological pattern of vegetation.

3.3. Effect of mining activities on NDVI

Fig. 10 shows NDVI trends in the Shenfu mining area and the # 4 planning area of the Yushen mining area, with a further statistical summary presented in Table 5. The Shenfu mining area is a currently mined area with association effects of natural conditions and mining activities on vegetation variations, while the # 4 planning area of the Yushen mining area is an unexploited area only with effect of natural conditions. The percentage differences of the decreased, unchanged, and increased areas between the unexploited areas and mined areas were 20.9269%, 16.5990%, and 4.3275%, respectively. In other words, the area percentage of vegetation ecological degradation caused by coal mining is 41.8534% higher than that of unexploited areas, which indicates that mining activities have an obvious negative impact on vegetation ecology. In order to accurately quantify the contributions of mining activities to vegetation changes, vegetation changes of the same mining area before and after mining will be detailly investigated in future research. Additionally, the aforementioned mining activities in the study refer to the full thickness mining of the coal seam and no water-preserved mining measures are implemented.

3.4. Determining the buried depth of the eco-safety groundwater table

Fig. 11 is a scatterplot showing the relationship between the depth of the groundwater table and mean NDVI values in 2014, which is characterized by a large number of data points and discreteness. The quantitative relationship between drought index and NDVI is shown in Eq. (9):

$$y_{NDVI} = 252.94853 \cdot x_{BDWL}^{0.22635} - 3365.99472 \cdot x_{BDWL}^{2} \cdot e^{-4.07404 x_{BDWL}} - 97.39793 \quad (9)$$

The correlation coefficient $R^2 = 0.9621$ is shown for the fit curve in Fig. 12, where y_{NDVI} is the mean NDVI value and x_{BDWL} is the depth of the groundwater table.

In Fig. 12, mean NDVI values increase with the depth of the groundwater table and reach a maximum when the groundwater table depth is 3 m. Afterwards, mean NDVI values gradually decrease with depth of the groundwater table. In detail, mean NDVI values increase from 0.27 to 0.35 in the areas of groundwater depth of 0–1.5 m, which is distributed around lakes and bottomlands with aquatic and hygrophilous vegetation. As the depth of the groundwater table increases, mean NDVI values increase from 0.35 to 0.43 in the areas of groundwater depths of 1.5–5.0 m, and aquatic and hygrophilous vegetation gradually shifts to mesophytic and xerophytic vegetation. When the depth of the groundwater table was 5.0–10.0 m, mean NDVI values decreased from 0.35 to 0.26, and the vegetation types were comprised of mainly mesophytic and xerophytic vegetation. When the depth of the groundwater table was greater than 10 m, the NDVI values were about 0.18, and the vegetation type was mainly xerophytic vegetation. Based on this pattern, the depth threshold of the groundwater level for vegetation in the study area was determined as follows. The depth of the

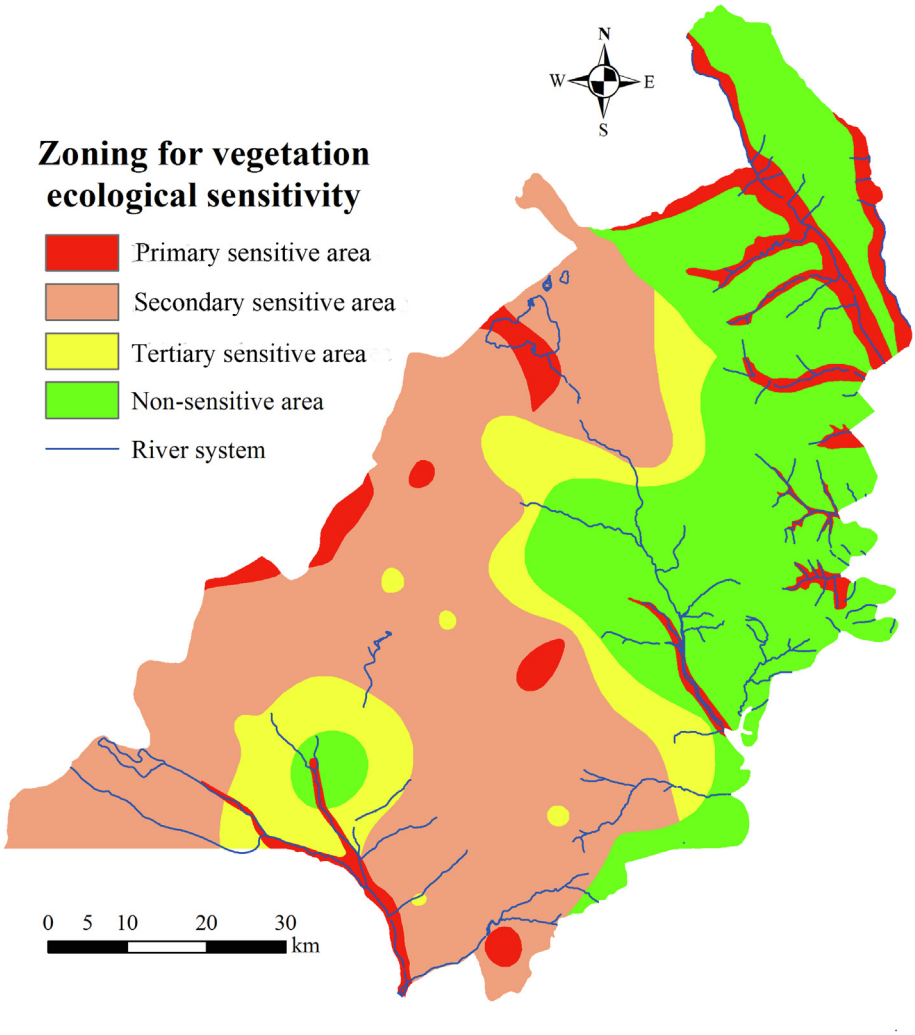

Fig. 13. Zoning map for vegetation ecological sensitivity.

groundwater level less than 1.5 m was identified as the water level depth limit for soil salinization. The groundwater level depth of 1.5–5.0 m was the water table depth consistent with the coexistence of hygrophytes and mesophytic and xerophytic vegetation. A groundwater depth of 5.0–10.0 m was the water level depth at which transitioned from mesophytic to xerophytic. A groundwater level depth greater than 10 m was only the groundwater level depth associated with xerophytic vegetation.

Therefore, the optimum groundwater table depth suitable for vegetation growth is 3 m, and the buried depth of the eco-safety groundwater table is 1.5–5.0 m in the Yushenfu mining area.

4. Discussion

During the 2006–2015 period, the geomorphic types and drought index values were basically unchanged, so geomorphic type and drought index had little influence on vegetation ecology. However, mining activities and groundwater depth have great influence on vegetation ecology. Mining activity has been the main driving factor of groundwater level changes (Fan et al., 2016). The water level monitoring points are mainly concentrated in the # 3 and # 4 planning areas of the Yushen mining area (i.e., un-mined areas; Fig. 1), where the groundwater level is basically unchanged. Because of the scarcity of water level monitoring points in the Shenfu mining area (i.e., mined areas), the impact of mining activities on groundwater is not monitored. Therefore, with the expected exploitation of the # 3 and # 4 planning areas in the Yushen mining area, the impact of groundwater level changes and mining activities on vegetation ecology can eventually be further analyzed. In order to provide more effective guidance for ecologists and mining engineers, zoning for ecological sensitivity is being implemented in the Yushenfu mining area.

In the study area, vegetation is mainly xerophytic. The vegetation growth depends on the groundwater only in the areas of shallow groundwater table depths, and changes in the groundwater table promote changes in vegetation ecology (Li et al., 2000; Ma et al., 2015). For this reason, based on the groundwater table depth threshold of 10 m, combined with topographic and geomorphic conditions, the vegetation ecological sensitivity of the study area is divided into sensitive and non-sensitive areas. In sensitive areas, according to the groundwater table depth threshold intervals, i.e., less than 1.5 m, 1.5–5.0 m, and 5.0–10.0 m, the area is further divided into three levels: primary, secondary, and tertiary sensitive areas. The groundwater table is deeper in the non-sensitive loess hilly and gully regions, and the native vegetation is therefore not affected by the groundwater. The groundwater depth in the river valley terrace is mostly less than 1.5 m, which corresponds to the primary sensitive area. The groundwater depth varies greatly in the blown-sand and beach area, and there are differences in sensitivity. Therefore, taking 1.5 m and 5.0 m as thresholds, further divisions based on ArcMap spatial analysis functions were determined in the blown-sand and beach area. Finally, vegetation ecological sensitivity was divided into four levels: primary, secondary, and tertiary sensitive areas and non-sensitive areas, as shown in Fig. 13.

The non-sensitive areas, secondary, and tertiary sensitive areas were mainly distributed in the eastern and northeastern parts, the western and southwestern parts, and the central and southern parts of the study area, respectively. The primary sensitive areas were scattered and mainly in the vicinity of the river system in the study area.

Different measures for protecting vegetation ecology should be implemented based the different ecologically sensitive areas. In the primary sensitive areas, the vegetation types are mainly aquatic and hygrophilous vegetation. The decline of groundwater level in these areas both promotes succession to xerophytic vegetation communities and reduces vegetation diversity, while promoting vegetation better suited to salinized land, which has positive and negative ecological effects on vegetation ecology in this area. Therefore, the groundwater can be utilized moderately by the local residents for both drinking water and irrigation. In secondary sensitive areas, the vegetation types are mainly mesophytic and hygrophilous. In tertiary sensitive areas, the vegetation types are mainly mesophytic and xerophytic. In general, the water flowing fractured zone height of mining activities should not penetrate into the phreatic aquifers in secondary and tertiary sensitive areas (Liu et al., 2018a, d; Qiao et al., 2017; Wang et al., 2017). Under these circumstances, strip mining and full filling mining methods are used to reduce the height of the water flowing fractured zone (Liu et al., 2018c; Zhang et al., 2009). In non-sensitive areas, the depth of the groundwater table is greater than 10 m and vegetation growth is maintained mainly by precipitation. The mining activities in these areas should be conducted in a way that ensures that there is no obvious subsidence on the surface (Chen et al. 2016; Wu et al., 2005), and afforestation activities should be conducted to improve the vegetation coverage.

Through the implementation of the aforementioned measures, the vegetation ecology environment and depth of groundwater can be basically unaffected by mining activities, and the control of the water flowing fractured zone height can also improve mining safety, which is of great significance for ecologists and mining engineers.

However, it is noted that there are several uncertainties in the present study. On one hand, although the calculated drought index can express the actual arid to semiarid climate condition, the shortage of meteorological stations has a certain effect on the calculation precision of drought index. Since the main objective of the paper was to study variation in vegetation, further studies on error analysis of calculation precision will be conducted in future research. On the other hand, vegetation variations are the comprehensive presentation of indicators such as mining activities, climate conditions, geomorphic types, and groundwater depth. With regard to the effect analysis of an indicator on NDVI, the uncertainty raising from other indicators may exist. In future research, the quantitative contribution of each indicator to vegetation variations should be strengthened.

5. Conclusions

Taking the Yushenfu mining area as a case study, the effects of geomorphology, groundwater depth, drought index, and mining activities on variation in vegetation among arid and semiarid mining areas were investigated. The vegetation ecology exhibited an increasing trend from 2006 to 2015 across the study area. The same geomorphology or the depth of the groundwater does not correspond to a determined NDVI value, and a relationship between the drought index and NDVI value was obtained. In contrast to the mining area that had been mined on a large scale, the area percentage of vegetation ecological degradation caused by coal mining is 41.8534% higher than that of unexploited areas, which indicates that mining activities have a negative impact on vegetation ecology.

Furthermore, areas of ecological sensitivity were identified. The ecological sensitivity division map was obtained for four zones based on the buried depth of the eco-safety groundwater table, i.e., the primary, secondary, and tertiary sensitive areas and non-sensitive areas. For different ecologically sensitive areas, different measures should be taken to protect the vegetation ecology.

Acknowledgements

This work was supported by the State Key Program of the National Natural Science Foundation of China [Grant number 41430643] and the National Basic Research Program of China (973 Program) [Grant number 2015CB251601].

Appendix A. Supplementary data

Supplementary data to this article can be found online at https://doi.org/10.1016/j.ecolind.2019.04.034.

References

Areola, M., Fasona, M., 2018. Sensitivity of vegetation to annual rainfall variations over Nigeria. Remote Sens. Appl.: Soc. Environ. 10, 153–162. https://doi.org/10.1016/j.rsase.2018.03.006.

Chen, W., Pourghasemi, H.R., Kornejady, A., Zhang, N., 2017a. Landslide spatial modeling: introducing new ensembles of ANN, MaxEnt, and SVM machine learning techniques. Geoderma 305, 314–327. https://doi.org/10.1016/j.geoderma. 2017.06.020.

Chen, X.Q., Wang, H., 2009. Spatial and temporal variations of vegetation belts and vegetation cover degrees in Inner Mongolia from 1982 to 2003. Acta Geogr. Sinica 64 (1), 84–94.

Chen, W., Xie, X.S., Peng, J.B., 2017b. GIS-based landslide susceptibility modelling: a comparative assessment of kernel logistic regression, Naïve-Bayes tree, and alternating decision tree models. Geomat. Nat. Haz. Risk 8 (2), 950–973.

Chen, S.J., Yin, D.W., Cao, F.W., Liu, Y., Ren, K.Q., 2016. An overview of integrated surface subsidence-reducing technology in mining areas of China. Nat. Hazards 81, 1129–1145. https://doi.org/10.1007/s11069-015-2123-x.

Chi, D.K., Wang, H., Li, X.B., Liu, H.H., Li, X.H., 2018. Assessing the effects of grazing on variations of vegetation NPP in the Xilingol Grassland, China, using a grazing pressure index. Ecol. Ind. 88, 372–383. https://doi.org/10.1016/j.ecolind.2018.01.051.

Christoffersen, B.O., Restrepo-Coupe, N., Arain, M.A., 2014. Mechanisms of water supply and vegetation demand govern the seasonality and magnitude of evapotranspiration in Amazonia and Cerrado. Agric. Forest Meteor. 191 (3), 33–50. https://doi.org/10.1016/j.agrformet.2014.02.008.

Demir, S., Abou-Jaoude, E., Kumral, M., 2017. Cognitive work analysis to comprehend operations and organizations in the mining industry. Int. J. Min. Sci. Technol. 27 (4), 605–609. https://doi.org/10.1016/j.ijmst.2017.05.008.

Deng, S.B., 2014. ENVI Remote Sensing Image Processing Method. Higher Education Press, Beijing, pp. 176–203.

Elmore, A.J., Manning, S.J., Mustard, J.F., 2006. Decline in alkali meadow vegetation cover in California: the effects of groundwater extraction and drought. J. Appl. Ecol. 43 (4), 770–779.

Fan, L.M., Xiang, M.X., Peng, J., Li, C., Li, Y.H., et al., 2016. Groundwater response to intensive mining in ecologically fragile area. J. China Coal Soc. 41 (11), 2672–2678.

Faour, G., Mhawej, M., Nasrallah, A., 2018. Global trends analysis of the main vegetation types throughout the past four decades. Appl. Geogr. 97, 184–195. https://doi.org/10.1016/j.apgeog.2018.05.020.

Gruijter, J.D., Brus, D., Bierkens, M., Knotters, M., 2006. Sampling for Natural Resource Monitoring. Springer, Berlin Heidelberg, pp. 189–190.

Gu, Z.J., Duan, X.W., Shi, Y.D., Li, Y., Pan, X., 2018. Spatiotemporal variation in vegetation coverage and its response to climatic factors in the Red River Basin, China. Ecol. Indic. 93, 54–64. https://doi.org/10.1016/j.ecolind.2018.04.033.

He, L., Shen, J., Zhang, Y., 2018. Ecological vulnerability assessment for ecological conservation and environmental management. J. Environ. Manage. 206, 1115–1125. https://doi.org/10.1016/j.jenvman.2017.11.059.

Jeevarathinam, C., Rajasekar, S., Sanjuán, M.A.F., 2013. Vibrational resonance in groundwater-dependent plant ecosystems. Ecol. Complex. 15 (5), 33–42.

Jiang, W.G., Yuan, L.H., Wang, W.J., Cao, R., Zhang, Y.F., Shen, W.M., 2015. Spatiotemporal analysis of vegetation variation in the Yellow River Basin. Ecol. Ind. 51, 117–126. https://doi.org/10.1016/j.ecolind.2014.07.031.

Jin, X., Xia, W., Guo, R., 2014. Variation of vegetation coverage in the Dulan area of Qaidam River Basin. J. Desert Res. 34 (2), 603–609.

Kendall, M.G., 1970. Rank Correlation Methods. Griffin, London.

Kong, D.X., Miao, C.Y., Borthwick, Alistair G.L., Lei, X.H., Li, H., 2018. Spatiotemporal variations in vegetation cover on the Loess Plateau, China, between 1982 and 2013: possible causes and potential impacts. Environ. Sci. Pollut. Res. https://doi.org/10.1007/s11356-018-1480-x.

Kopeć, D., Michalska-Hejduk, D., Krogulec, E., 2013. The relationship between vegetation and groundwater levels as an indicator of spontaneous wetland restoration. Ecol. Eng. 57 (6), 242–251.

Lantican, M.A., Guerra, L.C., Bhuiyan, S.I., 2003. Impacts of soil erosion in the upper Manupali watershed on irrigated lowlands in the Philippines. Paddy Water Environ. 1, 19–26. https://doi.org/10.1007/s10333-002-0004-x.

Lei, S.G., Bian, Z.F., 2014. Research progress on the environment impacts from

underground coal mining in arid western area of China. Acta Geogr. Sinica 34 (11), 2837–2843.
Li, P.Y., Li, X.Y., Meng, X.Y., Li, M.N., Zhang, Y.T., 2016. Appraising groundwater quality and health risks from contamination in a semiarid region of northwest China. Expos. Health 8 (3), 361–379.
Li, J.J., Peng, S.Z., Li, Z., 2017a. Detecting and attributing vegetation changes on China's Loess Plateau. Agric. For. Meteor. 247, 260–270.
Li, P.Y., Tian, R., Xue, C., Wu, J., 2017b. Progress, opportunities, and key fields for groundwater quality research under the impacts of human activities in China with a special focus on western China. Environ. Sci. Pollut. Res. 24 (15), 13224–13234.
Li, W.P., Ye, G.J., Zhang, L., Duan, Z.H., 2000. Study on the geological conditions of water conservation mining engineering in Yushenfu mining area in Northern Shaanxi. J. China Coal Soc. 25 (5), 449–454.
Liu, J.M., 1999. Hydrology and Water Resources Science. China Forestry Publishing House, Beijing, pp. 149–150.
Liu, S.L., Li, W.P., Wang, Q.Q., Pei, Y.B., 2018e. Investigation on mining-induced fractured zone height developed in different layers above Jurassic coal seam in western China. Arab. J. Geosci. 11 (2), 1–10. https://doi.org/10.1007/s12517-018 -3383-z.
Liu, S.L., Li, W.P., Wang, Q.Q., He, J.H., Xue, S., 2018d. Water inrush risk zoning and water conservation mining technology in the shennan mining area, Shaanxi. China. Arab. J. Sci. Eng. 43, 321–333.
Liu, Y., Li, L.H., Chen, X., Zhang, R., Yang, J.M., 2018f. Temporal-spatial variations and influencing factors of vegetation cover in Xinjiang from 1982 to 2013 based on GIMMS-NDVI$_{3g}$. Global Planet. Change 169, 145–155. https://doi.org/10.1016/j.gloplacha.2018.06.005.
Liu, S.L., Li, W.P., Wang, Q.Q., 2018b. Height of the water-flowing fractured zone of the Jurassic coal seam in northwestern China. Mine Water Environ. 37, 312–321. https://doi.org/10.1007/s10230-017-0501-1.
Liu, S.L., Li, W.P., Wang, Q.Q., 2018c. Zoning method for environmental engineering geological patterns in underground coal mining areas. Sci. Total Environ. 634, 1064–1076.
Liu, X.M., Meng, X.R., 2018. Evaluation and empirical research on the energy efficiency of 20 mining cities in Eastern and Central China. Int. J. Min. Sci. Technol. https://doi.org/10.1016/j.ijmst.2018.01.002.
Liu, R., Xiao, L.L., Liu, Z., Dai, J.C., 2018a. Quantifying the relative impacts of climate and human activities on vegetation changes at the regional scale. Ecol. Ind. 93, 91–99. https://doi.org/10.1016/j.ecolind.2018.04.047.
Lu, J., 2007. The least square method and its application. Sci. Tech. Western China 12, 19–21.
Ma, X.D., Fan, L.M., Zhang, X.T., Xiang, M.X., Liu, H.N., Zhang, Y.F., 2015. Dynamic changes of desertification landscape pattern at Yushenfu mining area in Yulin city of Shaanxi province. J. Catastrophol. 30 (4), 126–129.
Mao, F., Hou, Y.Y., Tang, S.H., Zhang, J.H., Lu, Z.G., 2007. Classification and dynamic changes of grasslands in northern Tibet based on recent 20 years satellite data. Chinese J. Appl. Ecol. 18 (8), 1745–1750.
Marques, M., Bienes, R., Pérez-Rodríguez, R., Jiménez, L., 2008. Soil degradation in central Spain due to sheet water erosion by low-intensity rainfall events. Earth Surf. Process. Landf. 33, 414–423. https://doi.org/10.1002/esp.1564.
Mathew, A., Khandelwal, S., Kaul, N., 2018. Spatio-temporal variations of surface temperatures of Ahmedabad city and its relationship with vegetation and urbanization parameters as indicators of surface temperatures. Remote Sens. Appl.: Soc. Environ. 11, 119–139. https://doi.org/10.1016/j.rsase.2018.05.003.
Minami, M., Sakala, J., Wrightsell, J., 2000. Using ArcMap. ESRI Inc., Redlands, USA.
Mou, N.X., 2012. ArcGIS10 Geography Information System Tutorial. Surveying and Mapping Press, Beijing, pp. 104–110.
Mu, X.H., Song, W.J., Gao, Z., McVicar, T.R., Donohue, R.J., Yan, G.J., 2018. Fractional vegetation cover estimation by using multi-angle vegetation index. Remote Sens. Environ. 216, 44–56. https://doi.org/10.1016/j.rse.2018.06.022.
Musa, H.D., Jiya, S.N., 2011. An assessment of mining activities impact on vegetation in Bukuru Jos Plateau state Nigeria using Normalized Differential Vegetation Index (NDVI). J. Sustain. Dev. 4 (6), 150–159.
Pei, Y.B., 2017. Eco-Geological Environment Type of Water Protection Coal Mining in Yushenfu Mining Area, Northern Shaanxi Province. China University of Mining and Technology, Xuzhou, pp. 31–32.
Pimentel, D., Kounang, N., 1998. Ecology of soil erosion in ecosystems. Ecosystems 1, 416–426. https://doi.org/10.1007/s100219900035.
Qiao, W., Li, W.P., Li, T., Chang, J.Y., Wang, Q.Q., 2017. Effects of coal mining on shallow water resources in semiarid regions: a case study in the Shennan Mining Area, Shaanxi. China. Mine Water Environ. 36, 104–113.
Ringrose, S., Chipanshi, A.C., Matheson, W., 2002. Climate and human-induced woody vegetation changes in Botswana and their implications for human adaptation. Environ. Manage. 30 (1), 98–109.
Rusanov, A.M., 2014. Recovery of natural vegetation and ecological functions of pasture ecosystems in arid steppes of the Cisural region. Russian J. Ecol. 45 (4), 243–248.
Sen, P.K., 1968. Estimates of the regression coefficient based on Kendall's tau. J. Am. Stat. Assoc. 63, 1379–1389.
Shi, C.X., Niu, K.Y., Chen, T.Z., Zhu, X.Y., 1986. Study on conversion coefficient of water surface evaporator. Scientia Geogr. Sinica 6 (4), 305–313.
Shiflett, S.A., Liang, L.L., Crum, S.M., Feyisa, G.L., Wang, J., Jenerette, G.D., 2017. Variation in the urban vegetation, surface temperature, air temperature nexus. Sci. Total Environ. 579, 495–505. https://doi.org/10.1016/j.scitotenv.2016.11.069.
Song, F.Q., Xing, K.X., Liu, Y., 2011. Monitoring and assessment of vegetation variation in Northern Shaanxi based on MODIS/NDVI. Acta Ecol. Sinica 31 (2), 354–363.
Stow, D., Daeschner, S., Hope, A., 2003. Variability of the Seasonally Integrated Normalized Difference Vegetation Index Across the North Slope of Alaska in the 1990s. Int. J. Remote Sens. 24 (5), 1111–1117.
Sun, X.C., Jin, X.M., Wan, L., 2008. Influence of groundwater on vegetation growth in Yinchuan plain. Modern Geol. 22 (2), 321–324.
Sun, Y.L., Yang, Y.L., Zhang, L., Wang, Z.L., 2015. The relative roles of climate variations and human activities in vegetation change in North China. Phys. Chem. Earth. 87–88, 67–78.
Symeonakis, E., Drake, N., 2004. Monitoring desertification and land degradation over sub-Saharan Africa. Int. J. Remote Sens. 25 (3), 573–592.
Tasser, E., Tappeiner, U., 2002. Impact of land use changes on mountain vegetation. Appl. Veg. Sci. 5 (2), 173–184.
Tian, F., Wang, Y.J., Fensholt, R., Wang, K., Zhang, L., Huang, Y., 2013. Mapping and evaluation of NDVI trends from synthetic time series obtained by blending Landsat and MODIS data around a coalfield on the Loess Plateau. Remote Sens. 5 (9), 4255–4279.
Tong, S.Q., Bao, Y.H., Zhang, Q.F., Du, W.L., 2016. Spatial and temporal variation of vegetation coverage in Inner Mongolia based on pixel dichotomy and intensity analysis. J. Ecol. Environ. 25 (5), 737–743.
Tosic, I., 2004. Spatial and temporal variability of winter and summer precipitataion over Serbia and Montenegro. Theor. Appl. Climatol. 77 (1), 47–56.
Turner, R.M., 1990. Long-term vegetation change at a fully protected sonoran desert site. Ecology 71 (2), 464–477.
United Nations Educational Scientific and Culture Organization, 1979. Map of the world distribution of arid regions: explanatory note. Man and Biosphere (MAB) Technical Notes, Paris.
United Nations Environment Programme, 1992. World Atlas of Desertification. UNEP, London.
Vereecken, H., Kollet, S., Simmer, C., 2010. Patterns in soil– vegetation – atmosphere systems: monitoring, modeling, and data assimilation. Vadose Zone J. 9, 821–827. https://doi.org/10.2136/vzj2010.0122.
Wan, Z.J., Wang, C.J., Qu, H., Liu, R., Zhang, Z.X., 2018. Vulnerability of forest vegetation to anthropogenic climate change in China. Sci. Total Environ. 621, 1633–1641. https://doi.org/10.1016/j.scitotenv.2017.10.065.
Wang, Y.J., 2017. Research progress and prospect on ecological disturbance monitoring in mining area. Acta Geod. Cartogra. Sinica 46 (10), 1705–17016.
Wang, H., Guo, Z.G., Xu, X.H., Liang, T.G., Ren, J.Z., 2007. Response of vegetation and soils to desertification of alpine meadow in the upper basin of the Yellow River, China. New Zealand J. Agric. Res. 50 (4), 491–501.
Wang, J., Wang, K.L., Zhang, M.Y., Zhang, C.H., 2015. Impacts of climate change and human activities on vegetation cover in hilly southern China. Ecol. Eng. 81, 451–461.
Wang, X.H., Wang, B.T., Xu, X.Y., Liu, T., Duan, Y.J., Zhao, Y., 2018b. Spatial and temporal variations in surface soil moisture and vegetation cover in the Loess Plateau from 2000 to 2015. Ecol. Ind. 95, 320–330. https://doi.org/10.1016/j.ecolind.2018.07.058.
Wang, G., Wu, M.M., Wang, R., Xu, H., Song, X., 2017. Height of the mining-induced fractured zone above a coal face. Eng. Geol. 216, 140–152. https://doi.org/10.1016/j.engge o. 2016.11.024.
Wang, G.F., Xu, Y.X., Ren, H.W., 2018a. Intelligent and ecological coal mining as well as clean utilization technology in China: review and prospects. Int. J. Min. Sci. Technol. https://doi.org/10.1016/j.ijmst.2018.06.005.
Webster, R., Oliver, M.A., 2008. Geostatistics for Environmental Scientists, second ed. John Wiley & Sons Ltd., Wiley, pp. 155–156.
Wu, L.X., Gao, J.H., Ge, D.Q., 2005. Experimental Study on Surface Subsidence Monitoring with D-InSAR in Mining Area. J. Northeastern Univ. (Nat. Sci.) 26 (8), 778–782.
Xie, Z.K., Zhang, M., 2018. Dynamic change regularity of ecosystem services in northern agro-pastoral ecotone with development of coal industry and coal-fired power generation. J. China Univ. Min. Technol. 47 (2), 436–442.
Xin, Z.B., Xu, J.X., Wei, Z., 2008. Spatiotemporal variations of vegetation cover on the Chinese Loess Plateau (1981–2006): impacts of climate changes and human activities. China Sci.: Earth Sci. 51 (1), 67–78.
Xu, M., Kang, S.C., Chen, X.L., Wu, H., Wang, X.Y., Su, Z.B., 2018. Detection of hydrological variations and their impacts on vegetation from multiple satellite observations in the Three-River Source Region of the Tibetan Plateau. Sci. Total Environ. 639, 1220–1232. https://doi.org/10.1016/j.scitotenv.2018.05.226.
Xu, J.X., Zhao, H., Li, G., Wu, L.X., Fu, J.C., 2017. Land ecological assessment and its spatial variation in coal mining area. J. China Univ. Min. Technol. 46 (1), 192–200.
Yang, Z.Y., Wang, W.K., Huang, J.T., Duan, L., 2006. Research on buried depth of ecosafety about groundwater table in the blown-sand region of the Northern Shaanxi Province. J. Northwest Agric. For. Univ.: Nat. Sci. Ed. 34 (8), 67–74.
Yang, X.H., Zhang, K.B., Hou, R.P., Ci, L.J., 2005. Vegetation variations under different exclusion measures and their correlation to soil factors. Acta Ecol. Sinica 25 (12), 3212–3219.
Zhang, Z.X., Chang, J., Xu, C.Y., Zhou, Y., Wu, Y.H., Chen, X., Jiang, S.S., Duan, Z., 2018. The response of lake area and vegetation cover variations to climate change over the Qinghai-Tibetan Plateau during the past 30 years. Sci. Total Environ. 635, 443–451. https://doi.org/10.1016/j.scitotenv.2018.04.113.
Zhang, M.S., Dang, X.Y., 2014. Water Resources and their Environmental Problems in Arid and Semi-Arid Regions. Science Press, Beijing, pp. 23–25.
Zhang, C.S., Hu, Y., Shi, X.L., 2016a. Analysis of spatial-temporal evolution of vegetation cover in loess plateau in recent 33 years based on AVHRR NDVI and MODIS NDVI. J. Appl. Sci. Electron. Inform. Eng. 34, 702–712. https://doi.org/10.969/j.issn.0255-8297.2016.06.006.
Zhang, F., Liu, X.P., Zhang, J.Q., Wu, R.N., Ma, Q.Y., Chen, Y.N., 2017a. Ecological vulnerability assessment based on multi-sources data and SD model in Yinma River Basin. China. Ecol. Mod. 349, 41–50.
Zhang, J.X., Miu, X.X., Guo, G.L., 2009. Development status of backfilling technology using raw waste in coal mining. J. Min. Safety Eng. 26 (4), 395–401.

Zhang, X.Q., Wang, L.K., Fu, X.S., Li, H., Xu, C.D., 2017c. Ecological vulnerability assessment based on PSSR in Yellow River Delta. J. Clean. Prod. 167, 1106–1111.
Zhang, G.L., Xu, X.L., Zhou, C.P., Zhang, H.B., Ou, Y.H., 2011. Responses of vegetation changes to vlimatic variations in Hulun Buir grassland in past 30 years. Acta Geogra. Sinica 66 (1), 47–58.
Zhang, Y., Zhang, C.B., Wang, Z.Q., Chen, Y.Z., Gang, C.C., An, R., Li, J.L., 2016b. Vegetation dynamics and its driving forces from climate change and human activities in the Three-River Source Region, China from 1982 to 2012. Sci. Total Environ. 563–564, 210–220.
Zhang, F.F., Zhang, H.Y., Evans, M.R., Huang, T.S., 2017b. Vegetation patterns generated by a wind driven sand-vegetation system in arid and semi-arid areas. Ecol. Complex. 31, 21–33. https://doi.org/10.1016/j.ecocom.2017.02.005.
Zhao, L., Dai, A.G., Dong, B., 2018. Changes in global vegetation activity and its driving factors during 1982–2013. Agr. For. Meteorol. 249, 198–209. https://doi.org/10.1016/j.agrformet.2017.11.013.
Zhao, A.Z., Zhang, A.D., Lu, C.Y., Wang, D.L., Wang, H.F., Liu, H.X., 2017. Spatiotemporal variation of vegetation coverage before and after implementation of Grain for Green Program was investigated in Loess Plateau. China. Ecol. Eng. 104, 13–22. https://doi.org/10.1016/j.ecoleng.2017.03.013.
Zhou, L., Tucker, C.J., Kaufmann, R.K., 2002. Variations in northern vegetation activity inferred from satellite data of vegetation index during 1981 to 1999. J. Geophys. Res. [Atmos.] 106 (D17), 20069–20083.